



# SPH Numerical Simulations of the Deformation of a Liquid Surface in Two Dimensions

Cristian Cáliz-Reyes<sup>1</sup>, Laura A. Ibarra-Bracamontes<sup>1</sup>,  
Rosanna Bonasia<sup>2</sup>✉, and Gonzalo Viramontes-Gamboa<sup>1</sup>

<sup>1</sup> Universidad Michoacana de San Nicolás de Hidalgo, Av. Francisco. J. Múgica  
S/N, C.U., 58030 Morelia Mich, Mexico  
laibarrab@gmail.com

<sup>2</sup> CONACYT-Instituto Politécnico Nacional, ESIA, UZ, Miguel Bernard,  
S/N, Edificio de Posgrado, 07738 Mexico City, Mexico  
rbonasia@conacyt.mx

**Abstract.** The Smoothed Particles Hydrodynamics (SPH) numerical method, DualSPHysics, was applied to simulate numerically the deformations generated when a solid object hits a liquid surface. In order to simplify the study, the simulations were carried out in 2D, with the hitting solid having a circular geometry. With the aim of comparing numerical and experimental results, a real quasi-2D cell was made using two acrylic walls with a 5 mm separation filled with water, using a slightly thinner Teflon disc as the hitting object. The simulation was able to reproduce qualitatively all the experimental phenomenology of the system, particularly the three main structures observed in the real quasi-2D (and also reported in 3D) situation: a crown splash, an air cavity, and a liquid jet. The maximum values reached by the depth of the cavity and the height of the jet were determined for two different impact velocities both numerically and experimentally. The numerical simulation better reproduced the experimental cavity depth than the jet height, with a percentage of average accuracy of 94% and 64% respectively. Accuracy was improved up to 85% for the maximum jet height when the effect of gravitational forces was increased and the maximum resolution was used in the numerical simulations. The differences found between experimental and simulation results can be attributed to the absence of a suitable model for surface tension in the single-phase system used to represent the free surface in the simulations, as well as to the confinement effects present in the experiments.

**Keywords:** SPH model · Splash deformation

## 1 Introduction

The deformation generated in a liquid surface either by the impact of a solid object or by a liquid is known as splash. Associated with the splash, a series of movements on the liquid surface can be identified. For example, if a solid object striking perpendicular to the liquid surface generates the deformation, the impact causes a release of liquid on the

surface forming what is known as a splash crown. Subsequently, the solid object descends displacing the liquid in its path and forming a hole called the air cavity. Finally, when the air cavity is closed due to the hydrostatic pressure exerted by the liquid, a jet is generated and expelled from the surface, which is defined as the liquid jet.

The splash is a phenomenon associated with fluid mechanics and shows the response of a liquid surface due to the energy transferred by the impact of an object. It is a common phenomenon in nature and can occur in industrial phenomena that handle liquids. For example, its study is of a great interest in industries dealing with ink injection printers. Some studies have been developed for the applications of the splash phenomenon in naval architecture, in the design of seaplanes, as well as in the military area for the development of missiles [23]. Some other works have focused on the analysis of the most appropriate way to enter the water during diving to avoid damage to the body; moreover, few related works try to understand how some basilisk lizards and shorebirds can walk on the surface of the sea [9].

Various experimental, theoretical and numerical studies, have been carried out in relation to the splash phenomenon. Among the numerical works is the one made by Alam et al. [1] that used the Semi-Implicit Particle Movement technique to determine the deformation of the splash crown by the vertical impact of a wedge in 2D. Wang et al. [24] used the numerical Border Integral Equation method to study the behavior of the air cavity formed by the impact of a wedge on the water surface. Other numerical studies, included within the Computational Fluid Mechanics, have been developed and applied to the splash phenomenon, based on Eulerian and Lagrangian methods [6, 10, 14].

The Smoothed Particles Hydrodynamics (SPH) is a meshless Lagrangian method that was developed to model continuous medium physics, avoiding the limitations of finite difference methods. It was applied for the first time forty years ago to solve astrophysical problems [8, 15]. The numerical method has proven to be robust and applicable to a wide variety of fields. For example, in the case of Fluid Dynamics, it has been applied in: multiphase flows [5, 18], gravity currents [17], free surface flow [19], sediment transport [26], among others. According to this method, the relevant physical quantities are calculated for each particle as an interpolation of the values of the nearest neighbor particles. The Lagrangian nature of the SPH method endows it with some advantages compared to the usual limitations of the Eulerian models. For example, there are no restrictions imposed either on the geometry of the system or the initial conditions, so that the latter can be easily programmed without the need for complicated grid algorithms such as those used in finite element methods. In addition, the number of particles increases in the regions where the fluid is present, in such a way that the computational effort is concentrated mainly in those regions and no time is wasted calculating the neighboring areas. The SPH model continues to evolve with new improvements in the approximations, stability and reliability of the model.

The code used in the present work, DualSPHysics [4], is an open source developed by a network of Universities. Thanks to the power of GPUs (graphics cards with parallel computing power), DualSPHysics can simulate real engineering problems using high resolution in a reasonable computing time. The code has already been used

to model the interaction of waves with floating bodies [2, 12], to analyze the upward movement of floating solids of different densities, and it has been validated with analytical models, experimental measurements and other numerical methods [7].

In this work, DualSPHysics is used to simulate the 2D deformations generated on a water surface as a result of the impact of a solid disc. First, physical experiments carried out to quantify splash magnitudes in a quasi-2D cell are described in general terms. Subsequently, the theoretical bases of the SPH method are presented. Finally, numerical simulations of physical experiments are described and results are compared with the experimental values. Limitations of the presented application of the numerical method and proposals for its improvement are discussed.

## 2 The Studied System

The goal of this research is to reproduce the deformations observed experimentally on a liquid surface hit by a solid object of circular cross section, using the DualSPHysics code.

The authors obtained experimental results in a simplified 2D system in a previous work [3]. The experimental values of the splash were obtained using a vertical rectangular quasi-two-dimensional cell. The volume available within the cell had the following dimensions: height  $H = 62$  cm, width  $W = 40.5$  cm and thickness  $E = 0.5$  cm. Distilled water was used as test liquid. To generate the deformations on the water surface, a Teflon disc of  $D = 2.54$  cm in diameter and a thickness  $e = 0.32$  cm was used. The solid disc was released in free fall from the top of the cell at a height  $Z$  above the water surface. The disc impact velocity on the liquid surface was controlled by varying the liquid level  $L$  within the quasi-2D cell. Figure 1 shows a diagram of the experimental cell with the mentioned variables to control the impact velocity. It is worth noting that the experiments described in Cáliz-Reyes et al. [3] were carried out within a cell of reduced thickness ( $E \ll H, W$ ), which produces confinement effects in the studied system. This implies that experimental results are affected by the presence of adjacent walls during the displacement of the disc when falling. This conditions imposes restrictions on the behavior of the disc, when it descends in a limited free fall, and in the response of the liquid during the induced deformations on its surface. Using image analysis, the maximum depth of the air cavity ( $H_c$ ) and the maximum height of the liquid jet ( $H_j$ ) were quantified. Figure 2 shows two of the characteristic fluid structures formed in the liquid surface during the splash [3]. To measure their magnitudes, the liquid level was taken as a reference before being deformed. Table 1 shows the experimental values that were taken into account in the numerical simulations, such as the water level and the impact velocity of the solid disc. Moreover, the maximum cavity depth and the maximum jet height, are also shown, for two impact velocity values.

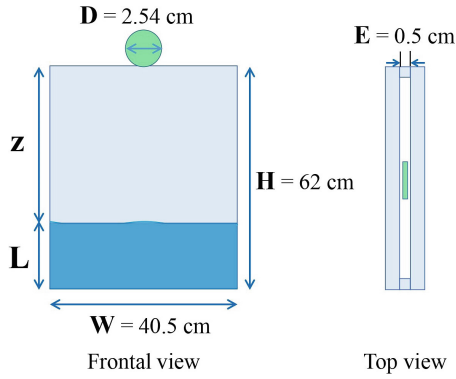


**Fig. 1.** Scheme of the physical model to generate the splash deformations on the liquid surface when impacting with a solid disc.

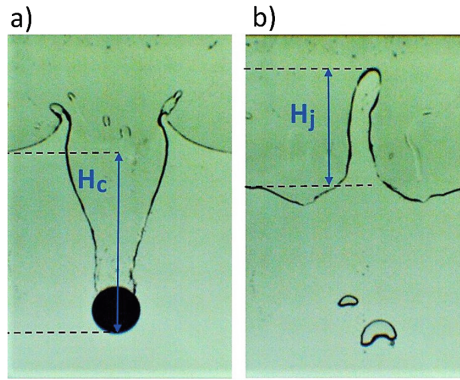


**Fig. 2.** Two of the fluid splash formations observed in the quasi-2D cell: (a) the air cavity; (b) the liquid jet. Both deformations are measured with respect to the free liquid surface level before the impact of the solid disc [3].

**Table 1.** Experimental values considered for the validation of the 2D simulation results. Values correspond to a quasi-2D splash generated using a solid disc of diameter  $D = 2.54$  cm [3].

Water level $L$ (cm)	Impact velocity $V_i$ (cm/s)	Maximum cavity depth $H_c$ (cm)	Maximum jet height $H_j$ (cm)
35	200	10.77	5.48
50	128	7.83	1.61

### 3 Methodology

#### 3.1 The DualSPHysics Model

The DualSPHysics code was designed for the numerical simulations of the experiments described in the previous section. The code has a pre-processing software that can use a wide range of input files for the creation of geometries. Advanced post-processing tools allow users to measure the physical magnitudes of any flow property at arbitrary locations within the domain.

The SPH method is based on integral interpolants so that the Navier-Stokes equations (governing equations of the model) are discretized using the kernel interpolation function. The governing functions are approximated as:

$$A(\vec{r}) = \int A(\vec{r}')W(\vec{r} - \vec{r}', h)d\vec{r}' \quad (1)$$

where  $h$  is the smoothing length and  $W(\vec{r} - \vec{r}', h)$  is the kernel (i.e. the weighting function). The integral interpolant can be expressed in discrete notation as:

$$A(\vec{r}) = \sum_b m_b \frac{A_b}{\rho_b} W_{ab} \quad (2)$$

where the summation applies to all particles (b) within the region defined by the kernel function ( $W_{ab} = W(\vec{r}_a - \vec{r}_b, h)$ ). The smoothing kernel function approximates a Dirac delta as the smoothing length tends to zero. It depends on the smoothing length and the non-dimensional distance between particles.  $m_b$  and  $\rho_b$  are mass and density respectively.

In DualSPHysics it is possible to choose between two types of kernel: Cubic Spline [16] and Quintic Wendland [25]. For the present work, the 5 degree smoothing kernel function was used.

For the solution of the momentum equation, DualSPHysics provides different options for the inclusion of the dissipation effect. In our experiments, the particle Reynolds number is of the order of  $10^4$ , being a value greater than the Reynolds number established for a laminar flow. This indicates that turbulent flows can be generated. For this reason, the laminar viscosity + Sub-Particle Scale (SPS) Turbulence model was used for the simulations proposed here. The concept of SPS [11] describes the effect of turbulence in the Moving Particle Semi-Implicit (MPS) model. The conservation equation is defined as:

$$\frac{dv}{dt} = -\frac{1}{\rho}\nabla P + g + v_0\nabla^2 v + \frac{1}{\rho} \cdot \vec{\tau} \quad (3)$$

where  $\vec{\tau}$  represents the SPS stress tensor. It is modeled using Favre-averaging (for a compressible fluid):

$$\frac{\tau_{ij}}{\rho} = -2\nu_t S_{ij} - \frac{2}{3}k\delta_{ij} - \frac{2}{3}C_I\Delta^2\delta_{ij}|S_{ij}|^2 \quad (4)$$

where  $\tau_{ij}$  is the sub-particle stress tensor,  $\nu_t$  is the turbulence eddy viscosity,  $k$  the SPS turbulence kinetic energy,  $C_I = 0.0066$ ,  $|S| = (2S_{ij}S_{ij})^{1/2}$ ,  $S_{ij}$  the element of SPS strain tensor. The laminar viscous term is treated as:

$$(v_0\nabla^2v)_a = \sum_b m_b \frac{4v_0r_{ab} \cdot \nabla_a W_{ab}}{(\rho_a + \rho_b)(r_{ab}^2 + \eta^2)} v_{ab} \quad (5)$$

where  $v_0$  is the kinematic viscosity (typically  $10^{-6}$  m<sup>2</sup>/s for water).

### 3.2 Numerical Simulations of the Physical Model

The numerical model seeks to represent the physical phenomenon that is observed on the surface of a liquid when it is impacted by a solid object of circular geometry. In order to simplify the system to a 2D model, a quasi-two-dimensional cell was used in the experimental system and a disc was used to generate the surface deformations in the water.

First, the computational domain was defined using two points in the space that allowed us to dimension the volume of the liquid to be studied in 3D. When the system is simplified to the 2D case, the numerical value assigned to one of the spatial coordinates, that is not taken into account, is repeated, generating a plane in space. For convenience, the  $XZ$  plane was chosen, where the  $X$  axis was located along the fluid interface, and the  $Z$  axis in the direction of the disc free fall.

In order to validate the numerical results, the conditions used in the experiments were implemented. For example, to define the volume of the liquid, the water level in the cell was considered along with the rest of the dimensions of the cell. A cylinder with a diameter of 2.54 cm and a thickness of 0.32 cm, was defined to represent the experimental disc, with the weight corresponding to the density of the material used (Teflon in this case). Once the disc geometry was generated, the property of the solid object was defined such that it could behave according to the rigid body dynamics. The magnitude and direction of the gravity force were indicated. The initial conditions of the liquid were defined such that the position and velocity of fluid particles represent an initial state of rest. The initial position of the disc and a zero initial velocity were also defined, so that once released, the disc would be subjected to the force of gravity and, on impact with the liquid surface, it would take a velocity of magnitude similar to the one obtained in the experiments.

As boundary conditions, a solid wall condition was established, both for the sidewalls and for the base of the computational domain. The shifting algorithm was included to take into account anisotropic particle spacing in regions close to the free surface or in violent flows. For the displacement of the solid disc, a dynamic boundary condition was used. According to this boundary condition, solid particles satisfy the same equations as fluid particles but do not move according to the forces exerted on them. Finally, for the fluid-solid interaction the fluid-driven object condition was

**Table 2.** Defined constants and parameters used in the numerical simulations.

<b>Constants</b>	
Particle assignment in the mesh	1 particle per node
Gravity	$-9.81 \text{ m/s}^2$ in the Z direction
Density	$1000 \text{ kg/m}^3$
Viscosity	$0.000001 \text{ m}^2/\text{s}$
Smoothing length coefficient (coefh)	1.2
Resolution (dp)	0.002 m
<b>Parameters</b>	
Precision	double
Time step algorithm	Symplectic
Smoothing Kernel	Wendland
Viscosity model	Laminar + SPS
Minimum time step (DtMin)	0.00001 s
Simulation time (TimeMax)	3 s

applied. This condition allows to derive the object movement by its interaction with fluid particles: the forces acting on each particle of the rigid body are computed according to the sum of the contribution of all surrounding fluid particles.

Table 2 shows some constants and parameters used for the numerical simulations. Parameters of interest, maximum depth of the cavity  $H_c$  and maximum height of the jet  $H_j$ , were measured with the Paraview software.

### 3.3 Simulations in 2D

For the 2D simulations, a computational domain was defined delimiting an XZ plane of dimensions  $W = 40 \text{ cm}$  wide and  $H = 62 \text{ cm}$  high, the same measures used in the experiments for the quasi-2D cell. The solid disc was defined in 2D as a solid circle of radius  $R = 1.27 \text{ cm}$ .

In the simulations the velocity at which the solid object impacts on the liquid surface was generated in a similar way as in the experiments: the disc was released from a certain height and fell by gravitational effects. Unlike in the experiments, the speed of the disc is affected by confinement and friction effects due to its proximity to the walls of the quasi-2D cell.

A convergence analysis was carried out for the resolution of the simulations in order to determine the adequate minimum distance between fluid particles (dp). By increasing the resolution, better numerical results should be obtained, but this in turn implies increasing the number of particles and consequently the computation time. The simulation resolution,  $dp$ , and the smoothing length are the variables that characterize the smoothing kernel, on which the performance of the SPH model strongly depends. Few studies have shown inconsistencies in the mathematical formalism of the kernel functions used in models like DualSPHysics, mainly due to errors inherent to the discretization of the equations or to truncation problems [20, 22]. Those effects are particularly evident when an interface between two phases is assumed. Moreover,

Korzani et al. [13] demonstrated that the ratio of the cylinder diameter to the initial distance between particles affects the simulations results. Taking all these considerations into account, we observed how certain fluid particles belonging to the free surface easily detached showing high velocities. This can be considered as a reflection of the instabilities that generate in the free surface, which can reduce the accuracy in the numerical results.

The experimental case used as reference is the one that corresponds to the impact velocity of the disc on the water surface  $V_i = 200$  cm/s, which generated a maximum jet height of  $H_j = 5.48$  cm, and a maximum cavity depth of  $H_c = 10.77$  cm (see Table 1).

The experimental impact velocity is the average value obtained from several experiments conducted under the same conditions [3]. In addition, the numerical value of the impact velocity is not an initial condition imposed in the simulation, it depends on the value of the height at which the disc was released. The numerical values of the impact velocity obtained in the simulations are within the range of variation of the corresponding experimental values.

Convergence in the numerical results depends on different factors, such as: resolution in simulation (related to the particle size), boundary conditions according to the phenomenon of interest, the main forces that describe the system behavior. For the latter case, the model proposed to deform the liquid surface shows some limitations. For example, the particles detected close to the free surface are only restricted in their diffusive movement towards low concentration regions, due to the high particle concentration gradient present at the interface.

Table 3 shows the results obtained in the 2D simulations by varying the resolution for a fixed impact velocity of the disc,  $V_i = 200$  cm/s. From the table, the numerical result for the maximum cavity depth shows a relative error percentage lower than 10% for all resolutions applied. But for a high simulation resolution ( $dp = 0.0008$  m), the height of the jet reaches a value of  $H_j = 9.9$  cm, which is sufficiently far from the value obtained experimentally. At lower resolution (e.g.  $dp = 0.002$  m), the jet height reaches the value of  $H_j = 6.1$  cm, which corresponds to a relative error percentage of 11%.

As particle size decreases, the gravitational force less affects the jet height, and a lower numerical convergence is obtained. Besides, due to the lack of a suitable model for the surface tension force, the growth of the liquid jet is overestimated. To overcome this situation, the gravitational forces were increased to compensate this effect. Table 3

**Table 3.** Numerical results for the maximum cavity depth and jet height obtained by varying the resolution in simulation and using an impact velocity of  $V_i = 200$  cm/s, some results consider increased gravitational forces ( $igf = 2$  g).

Simulation resolution, $dp$ (m)	Number of particles, $N_p$	Maximum cavity depth, $H_c$ (cm)	Maximum jet height, $H_j$ (cm)	Maximum cavity depth $igf$ , $H_{cg}$ (cm)	Maximum jet height $igf$ , $H_{jg}$ (cm)
0.0008	220,933	11.1	9.9	9.3	7.1
0.001	141,828	11.4	7.5	10	6.3
0.002	35,763	10.5	6.1	9.9	5.5
0.003	16,047	9.8	5.6	8.7	4.3



also shows numerical results for the case in which the gravitational forces are increased. Better results are obtained including a factor of 2 in the acceleration due to gravity (2 g) and a higher resolution. For example, with a resolution  $dp = 0.001$  m, the maximum jet height reaches a value of  $H_{jg} = 5.5$  cm, and the maximum cavity depth reaches a value of  $H_{cg} = 9.9$  cm. Both numerical results show a percentage of relative error lower than 10% with respect to the experimental results.

## 4 Results

### 2D Numerical Simulations of Liquid Surface Deformations Using Solid Walls as Boundary Conditions

The characteristic surface deformations of the splash that could be generated when a solid object hits a liquid are shown in Fig. 3. Numerical results show qualitatively the stages observed in the quasi-2D experiments. Three of the typical splash fluid structures are formed: a crown splash, an air cavity and a liquid jet. Both in the experiment and in the numerical simulation, the deformation in the surface of the liquid was induced upon impacting a solid disc with a velocity of approximately 250 cm/s.

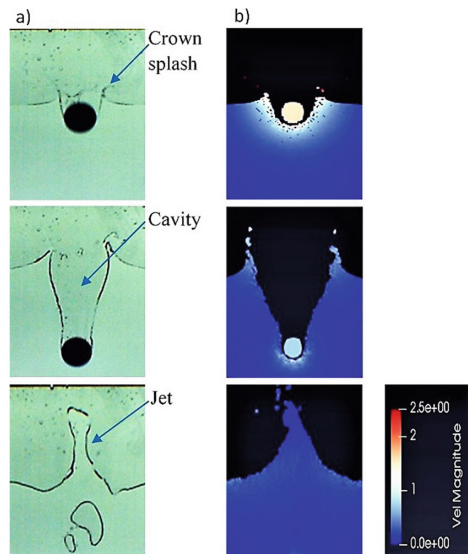


**Fig. 3.** Stages of the splash obtained from: (a) experiments in a quasi-2D cell; (b) 2D numerical simulations using DualSPHysics. The images correspond to the formation of the crown splash and the cavity during the entrance of the disc, and the ejection of the liquid jet. The color scale for the velocities in the numerical simulations is shown in m/s.

Table 4 shows a comparison between experimental and numerical values of the nondimensional maximum cavity depths and maximum jet heights.

Three cases are considered for comparison: Case 1 corresponds to an impact velocity  $V_i = 128$  cm/s with a simulation resolution of  $dp = 0.002$  m; Case 2 corresponds to an impact velocity  $V_i = 200$  cm/s with a simulation resolution of  $dp = 0.002$  m; Case 3 corresponds to an impact velocity  $V_i = 200$  cm/s with a simulation resolution of  $dp = 0.001$  m and increased gravitational forces. Furthermore, the respective Froude numbers, which relates the inertial forces to the gravitational forces, is also shown. The Froude number is generally expressed as:

$$Fr = \frac{V}{\sqrt{gl}} \quad (6)$$

In this system, its characteristic velocity ( $V$ ) was assumed as the impact velocity of the solid object ( $V_i$ ), and as the characteristic length ( $l$ ) the disc diameter ( $D$ ) was considered.

From Table 4, it can be seen that for a fixed value of the disc size, a decrease in the value of the Froude number corresponds to a lower impact velocity, while the maximum cavity depth and the jet height show a tendency to decrease.

Comparing experimental and numerical results for a fixed value of the impact velocity, a small difference in the maximum cavity depth, showing an error lower than 10% is observed. Therefore, the model reliably reproduces the formation of the cavity that provokes a deformation towards the interior of the liquid during the impact of the solid disc, transferring part of its kinetic energy to the fluid while the disc descends forming the cavity.

**Table 4.** Comparison between experimental and numerical nondimensional results for the maximum cavity depth and the maximum jet height, for two impact velocities, with  $D = 2.54$  cm.

	Experimental results	Numerical results	Experimental results	Numerical results	Numerical results
	$V_i = 128$ cm/s	Case 1	$V_i = 200$ cm/s	Case 2	Case 3
Nondimensional maximum cavity depth ( $H_c/D$ )	3.08	3.37	4.24	4.15	3.90
Nondimensional maximum jet height ( $H_j/D$ )	0.63	1.01	2.20	2.40	2.17
Froude number ( $Fr$ )	2.56	2.56	4.0	4.0	2.83

However, when comparing the results for the jet heights, the relative errors between numerical and experimental results increase. For example, in Case 1, for a lower impact velocity and a low resolution, the absolute differences are of the order of 1 cm. But jet height in Case 1 is of the order of a few centimeters, giving as result a relative error greater than 50%. In Case 2, the impact velocity is twice than the one applied in Case 1. Lower differences between experimental and numerical results for the jet height are

obtained at low resolution with a relative error of 10%. As the resolution increases (see Table 3), the maximum jet height differs more from the experimental result. Inertial forces are more dominant over gravitational and surface tension forces. Finally, in Case 3 the same impact velocity of the Case 2 is considered, and a greater gravitational force is imposed. This was done to compensate the lack of an explicit surface tension model and the low effect of gravitational forces when particle size is reduced as resolution increases. Better numerical results are obtained at a higher resolution than in Case 2, with a relative error of less than 5%. Even though the absolute differences between experimental and numerical results are of the order of 1 cm, the relative error is 15% for the highest resolution considered here.

Moreover, when the induced deformation causes an increase in the surface area in the opposite direction to gravity, surface instabilities occur and cause the fluid particles to detach at high velocity overcoming the surface tension forces. This low effect of surface tension forces could be one of the reasons why the jet grows to a greater extent than in the experiments. A similar phenomenon has already been observed when a sphere hits the surface of a granular medium generating a very high jet due to the absence of surface tension forces [21].

## 5 Conclusions

The SPH numerical model DualSPHysics was used to reproduce the deformations induced in a liquid surface by the impact of a solid object in two dimensions. The maximum cavity depth and the maximum jet height for fixed values of the impact velocity of the disc were calculated. Numerical results showed a good approximation to the experimental results, especially for the cavity depths. This allowed the validation of the DualSPHysics code for low impact speeds.

2D simulations were carried out applying solid walls as boundary conditions. Simulations qualitatively reproduced the deformations observed in the liquid free surface hit by a solid disc. In the range of values of Froude numbers considered here, between 2 and 5, inertial forces dominate over gravitational forces. This causes a great transfer of energy from the disc to the liquid at the impact moment, producing displacement of liquid and the opening of a cavity in the free surface. Due to the absence of a suitable model for surface tension in a single fluid phase system, and to the confinement conditions for 2D simulations, the numerically calculated jet height showed greater differences with respect to the experimental results at low impact velocities and high resolutions. In the experiments, the presence of nearby side walls contributes to fluid returning and to energy absorption that could affect the height of the emerging jet.

Numerical results should be improved incorporating a model that considers the effects of surface tension so to obtain a better representation of the interfacial deformations in a two-phase liquid-gas system.

**Acknowledgments.** Cáliz-Reye thanks CONACyT, UMSNH, and Santander scholarship by funding his research stay. Ibarra-Bracamontes would like to thank Andrew Belmonte for the collaborative work on the experimental results.

## References

1. Alam, A., Kai, H., Susuki, K.: Two-dimensional numerical simulation of water splash phenomena with and without surface tension. *J. Mar. Sci. Tech.* **12**, 59–71 (2007)
2. Bouscasse, B., Colagrossi, A., Marrone, S., Antuono, M.: Nonlinear water wave interaction with floating bodies in SPH. *J. Fluids Struct.* **42**, 112–129 (2013)
3. Cáliz-Reyes, C.: Analisis de la deformación en 2D de la superficie del agua al variar su tensión superficial durante la caída de un disco sólido (Unpublished master's thesis). Universidad Michoacana de San Nicolás de Hidalgo, Morelia, Mich. México (2019)
4. Crespo, A.J.S., et al.: DualSPHysics: open-source parallel CFD solver on Smoothed Particle Hydrodynamics (SPH). *Comput. Phys. Commun.* **187**, 204–216 (2015). <https://doi.org/10.1016/j.cpc.2014.10.004>
5. Cuomo, G., Panizzo, A., Dalrymple, R.A.: SPHH-LES two phase simulation of wave breaking and wave-structure interaction. In: *Proceedings: 30th International Conference on Coastal Engineering*, pp. 274–286 (2006)
6. Dou, P., Wang, Z., Ling, H.: Research method of the splash character of prismatic planing craft. *J. Har. Eng. Univ.* **39**(3), 422–427 (2018)
7. Fekken, G.: Numerical simulation of free surface flow with moving rigid bodies. Ph.D. thesis, University of Manchester, United Kingdom (2004)
8. Gingold, R.A., Monaghan, J.J.: Smoothed Particle Hydrodynamics: theory and application to non-spherical stars. *Mon. Not. R. Astr. Soc.* **181**, 375–389 (1977)
9. Glasheen, J., Macmahon, T.: Vertical water entry of disks at low Froude numbers. *Phys. Fluids* **8**(8), 2078–2083 (1996)
10. Gorla, C., Concli, F., Stahl, K., et al.: Simulations of Splash Losses of a Gearbox. *Adv. Tribol.* (2012) <https://doi.org/10.1155/2012/616923>
11. Gotoh, H., Shao, S., Memita, T.: SPH-LES model for numerical investigation of wave interaction with partially immersed breakwater. *Coast. Eng. J.* **46**(1), 39–63 (2001)
12. Hadžić, I., Henning, J., Peric, M., Xing-Kaeding, Y.: Computation of fluid-induced motion of floating bodies. *Appl. Math. Model.* **29**, 1196–1210 (2005)
13. Korzani, M.G., Galindo-Torres, S.A., Scheuermann, A., Williams, D.J.: Parametric study on smoothed particle hydrodynamics for accurate determination of drag coefficient for a circular cylinder. *Water Sci. Eng.* **10**(2), 143–153 (2017)
14. Li, M., Li, Q., Kuang, S., Zou, Z.S.: Computational investigation of the splashing phenomenon induced by the impingement of multiple supersonic jets onto a molten slag-metal bath. *Ind. Eng. Chem. Res.* **55**(12), 3630–3640 (2016)
15. Lucy, L.: A numerical approach to testing the fission hypothesis. *J. Astron.* **82**, 1013–1924 (1977)
16. Monaghan, J.J., Lattanzio, J.C.: A refined method for astrophysical problems. *Astron. Astrophys. Edp Sci.* **149**(1), 135–143 (1987)
17. Monaghan, J.J., Cas, R.F., Kos, A., Hallworth, M.: Gravity currents descending a ramp in a stratified tank. *J. Fluid Mech.* **379**, 39–70 (1999)
18. Monaghan, J.J., Kocharyan, A.: SPH simulation of multi-phase flow. *Comput. Phys. Commun.* **87**, 225–235 (1995)
19. Monaghan, J.J., Kos, A.: Solitary waves on a cretan beach. *J. Waterw. Port Coast. Ocean Eng.* **125**, 145–154 (1999)
20. Sigalotti, L., et al.: A new insight into the consistency of Smoothed Particle Hydrodynamics. *Appl. Math. Comput.* **356**, 50–73 (2019)
21. Thoroddsen, S.T., Shen, A.: Granular jets. *Phys. Fluids* **13**, 4–6 (2001)

22. Vaughan, G.L., Healy, T.R., Bryan, K.R., Sneyd, A.D., Gorman, R.M.: Completeness, conservation and error in SPH for fluids. *Int. J. Numer. Meth. Fluid.* **56**, 37–62 (2008)
23. Vincent, L., Xiao, T., Yohann, D., Jung, S., Kanso, E.: Dynamics of water entry. *J. Fluid Mech.* **846**, 508–535 (2018)
24. Wang, J., Lugni, C., Faltinsen, O.M.: Experimental and numerical investigation of a freefall wedge vertically entering the water surface. *Appl. Ocean Res.* **51**, 181–203 (2015)
25. Wendland, H.: Piecewise polynomial, positive definite and compactly supported radial functions of minimal degree. *Advances in Computational Mathematics*, vol. 4, pp. 389–396. Baltzer Science Publishers, Baarn/Kluwer Academic Publishers (1995). <https://doi.org/10.1007/BF02123482>
26. Zou, S., Dalrymple, R.A.: Sediment suspension simulation under flow with SPH-SPS method. In: *Proceedings: 30th International Conference on Coastal Engineering* (2006)